Pharm Res (2015) 32:1864–1883
DOI 10.1007/s11095-014-1581-2

RESEARCH PAPER

Development and Application of a Mechanistic Pharmacokinetic Model for Simvastatin and its Active Metabolite Simvastatin Acid Using an Integrated Population PBPK Approach

Nikolaos Tsamandouras • Gemma Dickinson • Yingying Guo • Stephen Hall • Amin Rostami-Hodjegan • Aleksandra Galetin • Leon Aarons

Received: 11 September 2014 / Accepted: 14 November 2014 / Published online: 2 December 2014

ABSTRACT

Purpose To develop a population physiologically-based pharmacokinetic (PBPK) model for simvastatin (SV) and its active metabolite, simvastatin acid (SVA), that allows extrapolation and prediction of their concentration profiles in liver (efficacy) and muscle (toxicity).

Methods SV/SVA plasma concentrations (34 healthy volunteers) were simultaneously analysed with NONMEM 7.2. The implemented mechanistic model has a complex compartmental structure allowing inter-conversion between SV and SVA in different tissues. Prior information for model parameters was extracted from different sources to construct appropriate prior distributions that support parameter estimation. The model was employed to provide predictions regarding the effects of a range of clinically important conditions on the SV and SVA disposition.

Results The developed model offered a very good description of the available plasma SV/SVA data. It was also able to describe previously observed effects of an OATP1B1 polymorphism (c.521 T > C) and a range of drug-drug interactions (CYP inhibition) on SV/SVA plasma concentrations. The predicted SV/SVA liver and muscle tissue concentrations were in agreement with the clinically observed efficacy and toxicity outcomes of the investigated conditions.

Conclusions A mechanistically sound SV/SVA population model with clinical applications (*e.g.*, assessment of drug-drug interaction and myopathy risk) was developed, illustrating the advantages of an integrated population PBPK approach.

KEY WORDS "drug-drug interactions" · "OATP1B1" · "PBPK" · "population model" · "simvastatin"

ABBREVIATIONS

AUC	Area under the concentration-time curve
CLR	Clarithromycicn
Cmax	Maximum concentration
CYP	Cytochrome P450
DDIs	Drug-drug interactions
DTZ	Diltiazem
ERY	Erythromycin
F	Oral bioavailability
F_a	Fraction absorbed into gut wall
F_g	Fraction reaching gut wall that escapes intestinal first-pass metabolism
F_h	Fraction reaching liver that escapes hepatic first-pass metabolism
F_{REC}	Parameter that quantifies the magnitude of the recycling (inter-conversion) process
FOCE-I	First order conditional estimation method with interaction
HMG-CoA	3-hydroxy-3-methylglutaryl-coenzyme A
IMPMAP	Monte-Carlo importance sampling assisted by mode a posteriori estimation
ITZ	Itraconazole
IVIVE	*In vitro - in vivo* extrapolation

Electronic supplementary material The online version of this article (doi:10.1007/s11095-014-1581-2) contains supplementary material, which is available to authorized users.

N. Tsamandouras (✉) • A. Rostami-Hodjegan • A. Galetin • L. Aarons
Centre for Applied Pharmacokinetic Research, Manchester Pharmacy School, The University of Manchester, Stopford Building, Room 3.32, Oxford Road, Manchester M13 9PT, UK
e-mail: nikolaos.tsamandouras@manchester.ac.uk

G. Dickinson • Y. Guo • S. Hall
Eli Lilly and Company, Indianapolis, Indiana, USA

A. Rostami-Hodjegan
Simcyp Limited, Blades Enterprise Centre, Sheffield, UK

IW	Inverse-Wishart distribution
LDL	Low-density lipoprotein
LOQ	Limit of quantification
MAP	Maximum a posteriori
MCMC	Markov chain Monte Carlo
OATP	Organic anion transporting polypeptide
PBPK	Physiologically-based pharmacokinetic
PK/PD	Pharmacokinetic/pharmacodynamic
RSE	Relative standard error
SNP	Single nucleotide polymorphism
SV	Simvastatin (lactone form)
SVA	Simvastatin acid (acid form)
VPC	Visual predictive check

INTRODUCTION

Simvastatin is a HMG-CoA reductase inhibitor, commonly used to treat lipid disorders and reduce the probability of a cardiovascular event in high-risk individuals [1,2]. It is administered in an inactive lactone form (SV) which needs conversion to simvastatin acid (SVA) in order to become active [3]. This conversion can be achieved non-enzymatically by hydrolysis and enzymatically by carboxylesterases present in different tissues (especially liver and small intestinal wall) and by paraoxonases in plasma [4]. Although the conversion of the lactone (SV) to the acid (SVA) form is predominant [4], SVA can be back-converted to SV either *via* an acyl-glucuronide intermediate that undergoes spontaneous cyclisation or *via* a coenzyme A-dependent pathway [5]. In addition to this complex inter-conversion process, both SV and SVA undergo CYP3A4/5 oxidative metabolism [6,7]. Due to the extensive hepatic and intestinal first-pass metabolism less than 5% of a SV dose reaches the systemic circulation [1].

The motivation to develop a model that accurately describes the complex SV/SVA pharmacokinetics derives mainly from the fact that the risk of muscle toxicity (the most serious adverse effect of the drug) is at least partly of a pharmacokinetic origin [8]. More specifically factors such as high dose, concomitant administration of drugs that interact with SV/SVA at the pharmacokinetic level (*e.g.*, CYP3A inhibition) and a polymorphism in the gene coding for the OATP1B1 hepatic uptake transporter (*SLCO1B1* c.521 T>C, or rs4149056) substantially increase the risk for myopathy [8]. Recently, we have published a population pharmacokinetic model focusing on the pharmacogenetics of simvastatin and the simultaneous identification of several polymorphisms and demographic characteristics that affect SV/SVA pharmacokinetics [9]. Although the reported model was adequate for the purpose of investigation, its empirical structure and data-driven nature could be seen as a limitation. In the absence of data from patients receiving the drug in other conditions and without having access to drug tissue concentrations, the model cannot extrapolate outside the studied population, or indicate the effects of certain conditions and population characteristics on drug tissue concentrations. Therefore, the aim of the current work was to develop a complex mechanistic population SV/SVA model with a physiologically-based structure that allows model predictions in the clinically relevant tissues, namely liver (site of efficacy) and muscle (site of toxicity). Such a model can be a valuable tool to extrapolate and predict the effects of myopathy predisposing conditions, such as genetic polymorphisms or drug-drug interactions (DDIs) on the disposition of SV and SVA, using *in vitro* data.

PBPK models are often used for exploratory simulations of concentration profiles during the drug development process and they are rarely used to analyse observed clinical data. This can be mainly attributed to the fact that parameter estimation in such complex models is a challenging task with many related methodological issues which we have recently reviewed [10]. It has been strongly recommended lately to combine PBPK with hierarchical population modelling in order to allow predictions not only at the individual but also at the population level [10,11]. Parameter estimation in such models should be performed without neglecting i) the variability in key system and drug related parameters and ii) the uncertainty on the results of *in vitro* experiments or *in silico* predictions that are used to inform model parameters. Therefore the current work aims also to serve as an example of an integrated population PBPK approach for the analysis of clinical data (*i.e.* combining so called "bottom-up" and "top-down" paradigms). The complex pharmacokinetics of simvastatin and their clinical relevance provide an excellent case to illustrate the advantages of a mechanistically sound population model.

MATERIAL AND METHODS

Pharmacokinetic Data for Model Development

SV and SVA pharmacokinetic data from two clinical studies (Study 1 & 2) conducted by Eli Lilly and Company were pooled and used for model development. Each of the two study protocols were reviewed and approved by an ethical review board. The studies were conducted in accordance with all applicable regulatory and Good Clinical Practice guidelines and followed the ethical principles originating in the Declaration of Helsinki. All subjects signed an informed consent document prior to participation in the studies. The demographic characteristics of the participants, the sampling times design and the methodology used to determine SV and SVA plasma concentrations in the collected blood samples have been extensively described elsewhere [9]. Briefly,

Study 1 involved 16 healthy volunteers who received a 40 mg simvastatin dose followed by a second 40 mg dose 24 h later, with rich sampling through this 48-h period. Study 2 involved 18 healthy volunteers who received a single 20 mg simvastatin dose and were intensively sampled for a 24-h period.

Structure of the SV/SVA Physiologically-Based Model

A mechanistic model (16 compartments) was developed in order to simultaneously describe the pharmacokinetics of SV/SVA and the complex inter-conversion process between them (Fig. 1). The structure of the developed model is such that it retains a physiological-mechanistic nature only in the parts which are relevant to the desired modelling purpose. Therefore, the model includes a small intestinal wall, liver vascular, liver tissue, systemic blood, muscle and rest of the body compartments for both SV and SVA. In order to account for the dissolution and absorption processes of the orally administered SV, two stomach content and two small intestinal lumen compartments referring to the solid and dissolved drug have been additionally incorporated for SV. Further details with regard to the model structure, including all the model assumptions and the mass balance differential equations of the joint SV/SVA system are provided in Supplement 1.

Use of Prior Information in the Population PBPK Model

The parameters of the developed model are mechanistic in nature and describe actual physiological processes. Therefore, these parameters can be informed from physiological/biological knowledge, *in vitro* experiments and *in silico* predictions. The available clinical data are limited to plasma concentrations and are insufficient to inform the estimation of all

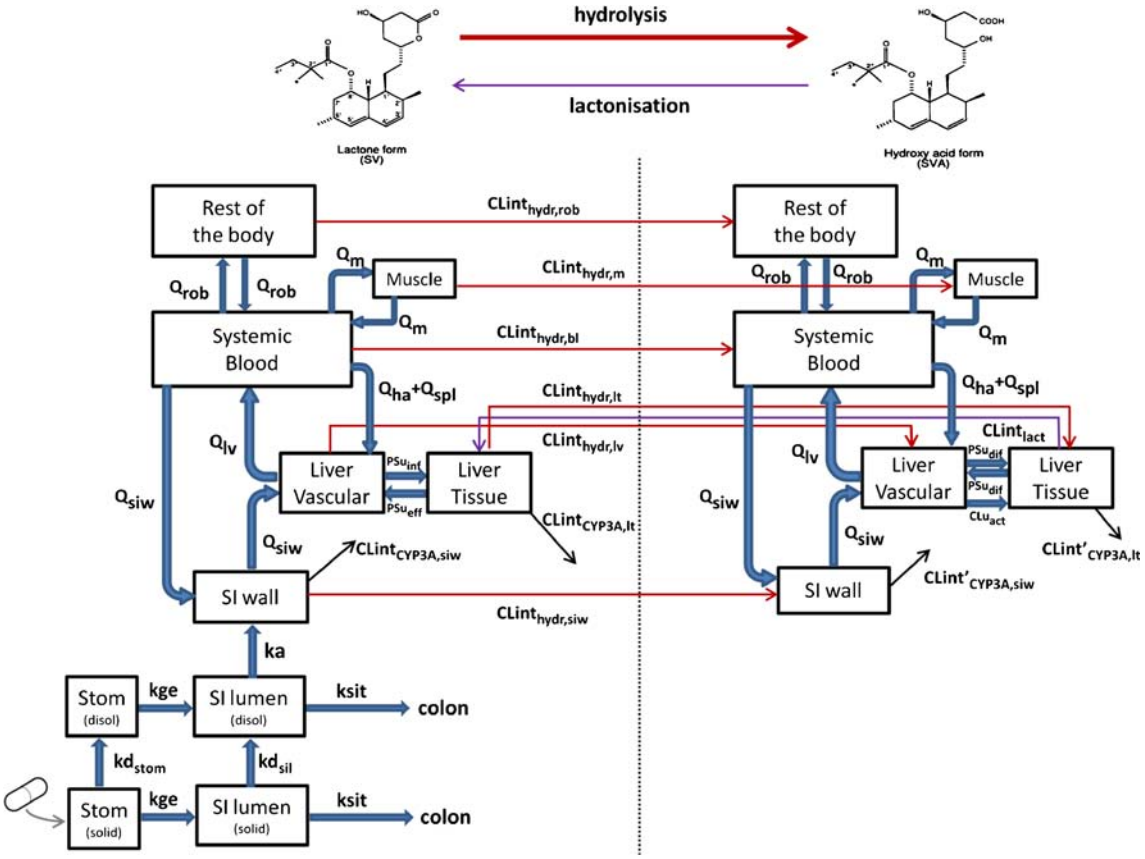

Fig. 1 Structure of the developed SV (left) / SVA (right) mechanistic model. Abbreviations: kd_{stom} dissolution rate constant in stomach contents, kd_{sil} dissolution rate constant in small intestinal lumen, *kge* gastric emptying rate constant, *ksit* small intestinal transit rate constant, *Stom* stomach content compartment, *SI lumen* small intestinal lumen compartment, *SI wall* Small intestinal wall compartment, *ka* absorption rate constant from the intestinal lumen into the epithelium, Q_{ha} hepatic artery blood flow, Q_m muscle blood flow, Q_{siw} small intestinal wall blood flow, Q_{rob} "rest of the body" compartment blood flow, Q_{spl} splachnic organs blood flow excluding small intestinal wall, Q_{lv} blood flow that exits the liver vascular compartment ($Q_{siw} + Q_{ha} + Q_{spl}$), PSu_{inf} *and* PSu_{eff} permeability surface product for unbound SV influx and efflux respectively across the basolateral membrane, PSu_{dif} passive diffusion clearance across the basolateral membrane for unbound SVA, CLu_{act} active uptake clearance for unbound SVA across the basolateral membrane, $CLint_{lact}$ intrinsic clearance for lactonisation in the liver tissue, $CLint_{CYP3A,i}$ intrinsic clearance for CYP3A mediated oxidative metabolism in compartment (i), $CLint_{hydr,i}$ intrinsic clearance for SV to SVA hydrolysis in compartment (i); the (i) subscripts bl, lt, lv, m, siw and rob represent the systemic blood, liver tissue, liver vascular, muscle, small intestinal wall and rest of body compartments respectively. When any of the above abbreviations is relevant to both SV and SVA, the abbreviation referring to SVA is followed by a prime.

complex model parameters. Therefore, it was prudent to combine the current clinical data with the available prior information in order to aid the parameter estimation process. In addition, the drug-related parameter values of this complex PBPK model are informed from *in vitro* experiments or *in silico* calculations and may be associated with a certain degree of inaccuracy and/or imprecision. Hence, in the current work the confidence in prior information related to model parameters was summarised in terms of appropriate statistical distributions allowing parameters to move during estimation, updating (if possible) prior knowledge with the clinical data from the current study. However, some model parameters still needed to be treated as fixed values particularly when the confidence around these values was high (*e.g.*, certain physicochemical properties, fractions unbound, blood to plasma ratios *etc.*) in order to reduce the dimensionality of the parameter estimation process. Prior information was considered during parameter estimation using the prior functionality [12,13] in NONMEM 7.2 (ICON Development Solutions, Ellicott City, MD). Briefly, in this method the objective function upon minimisation includes a penalty term which reflects a representation of the available prior knowledge with regards to model parameters. Such an approach differs from a typical Bayesian method in that it does not generate a posterior distribution of the parameter estimate, but rather outputs maximum a posteriori (MAP) point estimates.

Population Pharmacokinetic Analysis

Population pharmacokinetic modelling was performed using nonlinear mixed-effects modelling software (NONMEM, version 7.2). Additional investigations of the NONMEM output, model simulations, as well as the statistical and graphical analyses, were performed in Matlab R2012a (The MathWorks, Inc., Natick, Massachusetts, USA). The developed mechanistic model was coded as a system of 16 ordinary differential equations (see NONMEM code in Supplement 9). The differential equations were evaluated with ADVAN13, which corresponds to an LSODA differential equation solver that can handle a mixed system of both stiff and non-stiff differential equations. The population analysis was performed using the first order conditional estimation method with interaction (FOCE-I) and the results presented in this manuscript principally refer to this method. However, the need for decreased computation times for convergence in such a complex mechanistic model motivated also the evaluation of alternative estimation algorithms. Therefore, estimation was also performed with the Monte-Carlo importance sampling method assisted by mode a posteriori estimation, namely IMPMAP in NONMEM 7, parallelised in 7 cores of an Intel® Xeon® X5570 processor (2.93 GHz, 24 GB of RAM). Further information and practical details regarding the application and the set-up of this estimation method are provided in Supplement 2 (section 1).

In total 550 SV and 550 SVA concentration measurements in plasma derived from the two pharmacokinetic studies described above were analysed simultaneously. In that dataset, 41/550 SV and 90/550 SVA plasma concentration measurements were below the limit of quantification (LOQ) and these were substituted with (LOQ/2) [14]. The more sophisticated M3 method (a method that retains observations below the LOQ as censored data and maximizes the likelihood to predict these observations below the LOQ) [14], was not applied in the current work. Although this method is generally recognised as the optimal way to treat data below the LOQ, it was not feasible here due to the complexity of the model which would lead to unacceptable long runtimes. However, the selected approach to treat data below the LOQ was further validated with a visual predictive check (VPC) variation in which the agreement between the fraction of observed and model-predicted concentrations below the LOQ can be also examined [15]. The residual unexplained variability was modelled for both SV and SVA concentrations with an additive error model on the log-transformed data (equivalent to an exponential error model on the un-transformed data). No prior information was provided with regard to the residual variability random effect terms.

The structural model parameters can be classified as system-related and drug-related. The former were considered known at the fixed effect (typical individual) level, based on physiological/biological information. An overview of the physiological system-related parameter values of the model is provided in Table I. All the system-related parameters and their population variability are extensively described in Supplement 3. An overview of the drug-related parameters, their assigned values when they are considered fixed and their assigned prior distributions when they are to be estimated are provided in Table II. All the drug-related model parameters, the derivation of their prior distributions and the stochastic model regarding their population variability are extensively described in Supplement 4.

The structural model parameters which are upon estimation were log-transformed (the natural log of the parameters was estimated) to allow sampling of the log-parameters from the multivariate normal that has been assigned for the priors related to the fixed effects [16] (see NONMEM code in Supplement 9). Moreover, in this way negative values for the parameters in the untransformed domain are avoided. In total 14 drug-related parameters (fixed effects) were estimated. For the majority of these parameters (10 out of 14) informative priors were provided (Table II) and parameter estimation was performed at the level of the prior knowledge (*e.g.*, at the level of intrinsic rather than whole hepatic clearance) to minimise as much as possible additional transformations of the prior distributions (see Supplement 4 section 1 for further discussion). The remaining 4 parameters were estimated solely from the data due to the lack of any prior knowledge. For these parameters, uninformative priors were provided by setting the

Table I System-Related Parameter Values Applied to the SV/SVA Pharmacokinetic Model

Parameter	Value	Reference [a]
f_{siw}	0.0091	Literature
f_{lt}	0.0257	Literature
f_{lv}	0.00296	Literature [b]
f_{bl}	0.0743	Literature
f_{m}	0.4	Literature
f_{spl}	0.0114	Literature [c]
f_{rob}	0.4765	Calculated [d]
R_{sil} (cm)	1.61	Calculated [e]
kge (h^{-1})	4	Literature [f]
ksit (h^{-1})	0.28	Literature [f]
q_{siw}	0.105	Literature
q_{ha}	0.065	Literature
q_{m}	0.145	Literature
q_{spl}	0.095	Literature [g]
q_{rob}	0.590	Calculated [h]
V_{stom} (L)	0.05	Literature
V_{sil} (L)	0.608	Literature

f_i represents the fractional volume of tissue-compartment (i) with respect to total body weight; q_i represents the fractional blood flow of tissue-compartment (i) with respect to the cardiac output; subscripts bl, lt, lv, m, siw, ha, spl and rob are referring to systemic blood, liver tissue, liver vascular, muscle, small intestinal wall, hepatic artery, "rest of splachnic" and "rest of body" respectively. For example the muscle tissue in the model represents 40% of the total body weight and it is receiving 14.5% of the cardiac output of an individual. V_{stom} and V_{sil} refer to the volume of stomach content and small intestinal lumen respectively; R_{sil} represents the radius of small intestinal lumen; kge and ksit represent the gastric emptying and small intestinal transit rate constants respectively. For further details on system-related model parameters see Supplement 3

[a] References for parameter values informed from literature are reported in Supplement 3 (see Table S3.1)

[b] The fractional volume of the liver vascular compartment has been calculated as 11.5% of the liver tissue fractional volume

[c] The fractional volume of the "rest of splachnic" compartment (see Supplement 1) has been calculated as the sum of the fractional volumes of stomach, large intestine, pancreas and spleen which are 0.0021, 0.0053, 0.0014 and 0.0026 respectively

[d] The fractional volume of the "rest of body" compartment has been calculated as 1 minus the sum of other fractional volumes in the model

[e] The reported radius of small intestinal lumen has been calculated as explained in Supplement 3 (Eqs. S3.4–S3.11) using the average weight and height of the individuals in the analysed datasets. Note that this is only a reference-typical value as this parameter is not fixed across the population (see Supplement 3)

[f] Note that the gastric emptying and the small intestinal transit rate constants reported here are only reference-typical values as these parameters are not fixed across the population (see Supplement 3)

[g] The fractional blood flow of the "rest of splachnic" compartment (see Supplement 1) has been calculated as the sum of the fractional blood flows of stomach, large intestine, pancreas and spleen which are 0.01, 0.045, 0.01 and 0.03 respectively

[h] The fractional blood flow of the "rest of body" compartment has been calculated as 1 minus the sum of other fractional blood flows in the model

variance of the normal prior that refers to the natural logarithm of the parameter of interest to the value of 10,000. This is equivalent to the standard value of 0.0001 that is used as the precision of an uninformative prior in Bayesian analyses. The identifiability of the structural model parameters is discussed in Supplement 4 (section 3).

With regard to the majority of the inter-individual variability random effect terms, prior information was unavailable. In this case, uninformative priors were designated by setting the degrees of freedom of the associated inverse-Wishart (IW) distributed prior equal to the dimension of each omega block [16] (see NONMEM code in Supplement 9). In the case of model parameters for which prior information regarding their population variability was available (*e.g.*, gastric and small intestinal residence times, see Supplement 3), informative priors were provided and the exact values of the associated IW degrees of freedom were calculated with the analytical expressions described by Dokoumetzidis and Aarons [17].

Covariate model building was not attempted as the aim of the current work was the development of a base population mechanistic model and all the individuals included in the analysis were healthy volunteers. However as explained in Supplement 3, total body weight and body surface area are *a priori* defined to affect some of the system-related model parameters (*e.g.*, organ volumes, cardiac output) with fixed covariate relationships. Genotype information was also available for these individuals for 18 genetic polymorphisms of seven genes (3, 3, 1, 1, 7, 2, and 1 polymorphisms in the *ABCB1*, *ABCG2*, *CYP3A4*, *CYP3A5*, *SLCO1B1*, *SLCO2B1*, and *PPARA* genes, respectively). However, the development of a population pharmacokinetic model with genetic covariates was the focus of a previous work [9] with a much larger sample size. However, it should be noted that none of the individuals studied in the current work was homozygous (CC) for the OATP1B1 c.521 T>C SNP (rs4149056), a genotype that has the highest impact on SVA pharmacokinetics and is acknowledged to play a clinically important role [8,18].

Model Validation

Evaluation of traditional PK/PD models usually consists of thorough diagnostics that mainly focus on how well the model describes the fitted data [19]. However, validation of a population physiological model, such as the one developed here, should be performed under a slightly different framework borrowing elements from the PBPK field [20]. This is firstly because the model structure and several parameter values are dictated from the underlying physiology and are not subject of model building. In addition, such models are mainly developed for their ability to perform extrapolation outside the studied conditions and not to solely describe the observed data [10,21]. In such a situation although a good description of the observed plasma concentration profiles is a good diagnostic of the model's performance, it is

Table II Drug-Related Parameter Values Applied to the SV/SVA Pharmacokinetic Model

Model parameter	SV	SVA	Reference
logP/log$D_{7.4}$	4.68	4.54/1.45	2.4, 2.5
ρ (g/mL)	1.2	–	2.1
D (cm^2/min)	$4.04 \cdot 10^{-4}$	–	2.1
h (μ)	9.18	–	2.1
r (μ)	9.18	–	2.1
Sol_{sil} (μg/mL)	16.4	–	2.1
Sol_{stom} (μg/mL)	14.5	–	2.1
BP	0.57	0.56	2.3
fu_{bl}	0.0235	0.0979	2.4
fu_{lt}	indirectly [b]	0.0919	2.4
fu_{lv}	0.0235	0.0979	2.4
fu_{m}	indirectly [b]	–	2.4
fu_{rob}	0.0264	–	2.4
fu_{siw}	1	1	2.4
$KPu_{T:P,lt}$	(7.344, 0.539)	–	2.5
$KPu_{T:P,m}$	(6.782, 0.539)	(0.476, 0.539)	2.5
$KP_{T:B,rob}$	(Uninformative) [a]	(Uninformative) [a]	2.5
P_{eff} (cm/h)	(0.437, 0.703) [a]	–	2.2
PSu_{dif} (L/h)	–	49.42	2.6
PSu_{inf} (L/h)	874200	–	2.6
PSu_{eff} (L/h)	874200	–	2.6
CLu_{act} (L/h)	–	(Uninformative) [a]	2.6
$CLint_{CYP3A,vitro}$ [c]	(3.124, 0.346) [a]	(−2.948, 0.094) [a]	2.7, 2.8
$k_{hydr,pl}$ (h^{-1})	(−2.214, 0.068)	–	2.9
$k_{hydr,buff}$ (h^{-1})	(−3.650, 0.0015)	–	2.9
$k_{hydr,S9}$ (h^{-1})	(−2.752, 0.0061)	–	2.9
$k_{hydr,hybrid}$ (h^{-1})	(Uninformative) [a]	–	2.9
$k_{lact,S9}$ (h^{-1})	–	0.0024	2.10
$CLint_{gluc,vitro}$ [d]	–	(−0.997, 0.108)	2.10

For the parameters which are upon estimation, the assigned prior distributions are described inside parentheses. When an informative prior has been assigned, the mean and variance (μ, σ^2) of the normal prior that refers to the natural logarithm of the parameter are reported. Parameter values not in parentheses are considered fixed. Further details regarding each parameter and the derivation of the assigned values/priors are provided in Supplement 4 and specifically in the section reported in the Reference column

ρ particle density, *D* diffusion coefficient, *h* diffusion layer thickness, *r* particle radius, Sol_{sil} *and* Sol_{stom} solubility in small intestinal lumen and stomach content compartments respectively, *BP* blood-to-plasma ratio, fu_{bl}, fu_{lt}, fu_{lv}, fu_{m}, fu_{rob} *and* fu_{siw} fraction unbound in blood, liver tissue, liver vascular, muscle, rest of body and small intestinal wall compartments respectively, $KPu_{T:P,lt}$ *and* $KPu_{T:P,m}$ tissue to plasma unbound partition coefficient for liver and muscle tissue respectively, $KP_{T:B,rob}$ tissue to blood partition coefficient for the rest of body compartment, P_{eff} effective permeability to the small intestinal wall, PSu_{dif} passive diffusion clearance across the basolateral membrane for unbound SVA, PSu_{inf} *and* PSu_{eff} permeability surface product for unbound SV influx and efflux respectively across the basolateral membrane, CLu_{act} active uptake clearance for unbound SVA across the basolateral membrane, $CLint_{CYP3A,vitro}$ *in vitro*-determined intrinsic CYP3A clearance, $k_{hydr,pl}$, $k_{hydr,buff}$ *and* $k_{hydr,S9}$ *in vitro*-determined hydrolysis rate constants in plasma, $buffer_{pH=7.4}$ (referring to muscle) and liver S9 respectively, $k_{hydr,hybrid}$ hybrid hydrolysis rate constant in the small intestinal wall and rest of body compartments, $k_{lact,S9}$, *in vitro*-determined lactonisation rate constant in liver S9 (referring to other than glucuronidation-mediated lactonisation), $CLint_{gluc,vitro}$ *in vitro*-determined intrinsic glucuronidation clearance (referring to glucuronidation-mediated lactonisation)

[a] Inter-individual variability terms were applied in these model parameters (see Supplement 4 section 4)

[b] These parameters are indirectly estimated as they are parameterised in terms of the directly estimated SV tissue partition coefficients in liver and muscle (see Supplement 4, Eq. S4.12)

[c] Expessed in μL/min/pmol of CYP3A for SV and mL/min/mg of microsomal protein (MP) for SVA

[d] Expressed in μL/min/mg of microsomal protein

not necessarily sufficient to demonstrate the model's adequacy. In the current work, validation of the developed mechanistic model was performed with the following steps. Firstly, as model parameters represent real physiological processes the parameter estimates were assessed in terms of their physiological/mechanistic plausibility. Secondly, model evaluation diagnostics

routinely used in population pharmacokinetic modelling (goodness of fit plots, VPC, bootstrapping procedure) were employed to assess the robustness of parameter estimates and the ability of the model to adequately describe the observed data and their variability (see Supplement 5 section 1 for further details). Subsequently, an independent (not fitted) dataset consisting of SV/SVA plasma concentrations determined in 28 healthy volunteers [22] was used for external model validation (see Supplement 5 section 2 for further details). Finally, the model was evaluated in terms of its predictive performance in situations outside of the studied population and conditions where some of the mechanisms of the system are perturbed (*e.g.*, genetic polymorphisms and DDIs), (see model applications below).

Simulation of SV/SVA Concentration Profiles and Determination of Additional Parameters of Mechanistic Interest

In addition to plasma, the developed model was used to predict concentration profiles of both forms in the other clinically relevant tissues which are the liver (site of action) and the muscle (site of toxicity). The typical population parameter estimates of the model and a weight and height of 70 kg and 170 cm respectively were used to perform these simulations. Furthermore, the developed population model was used to perform simulations and investigate additional parameters of mechanistic interest and the magnitude of their population variability. These included SV bioavailability (F) and its constituent components *i.e.*, the fraction absorbed into gut wall (F_a), the fraction reaching gut wall that escapes intestinal first-pass metabolism (F_g) and the fraction reaching liver that escapes hepatic first-pass metabolism (F_h); and finally the recycling fraction (F_{REC}), a parameter that quantifies the magnitude of the recycling (inter-conversion) process. The procedure to calculate these parameters and their population variability is described in Supplement 5 (section 3).

Applications of the Developed Model - Extrapolation

The developed population model was evaluated with regard to its potential for extrapolation in conditions where mechanisms of the developed system are perturbed. The investigated scenarios are related firstly to the effect of the clinically important polymorphism c.521 T>C (rs4149056) in the gene coding for the OATP1B1 transporter and secondly to a range of clinically important simvastatin DDIs, as described below.

Effect of the OATP1B1 c.521 T>C (CC) Genotype on SV and SVA Disposition

None of the individuals studied in the current work was homozygous (CC) for the OATP1B1 c.521 T>C SNP. Therefore, published data were digitally extracted (GetData Graph Digitizer 2.26) from a previous clinical study [18] in which mean SV/SVA plasma concentrations were available for both the homozygous wild type TT ($n=16$) and the homozygous variant CC ($n=4$) genotype. The first step was to assess the ability of the developed model to describe these observed data for the homozygous wild type TT group. Therefore a simulation was performed using the typical parameters of the developed mechanistic model and the mean population characteristics of the TT group in the reported clinical study (weight of 68 kg and height of 174 cm). The model simulated typical SVA plasma concentration profile was compared with the observed data to assess the degree of agreement.

Subsequently, conditionally on the success of this first step, the second aim was to assess the ability of the developed model to describe the observed SVA data for the homozygous variant CC group. If mechanistically correct, the developed model should have the ability to describe the observed data after only adjusting the model parameter where the genotype effect is manifested, *i.e.*, the SVA active uptake clearance (CLu_{act}). The mean population characteristics of the CC group in the reported study (weight of 84 kg and height of 180 cm) were used as model input. All the parameters of the developed model were fixed to the population-typical values and a single covariate parameter representing the *in vivo* effect of the CC genotype on SVA active uptake clearance was estimated using the observed mean SVA data of the CC group. Estimation of this single parameter was performed in Matlab R2012a using the *lsqnonlin* function and the "trust-region reflective" algorithm, which are designed to solve nonlinear least-squares curve fitting problems. The model-simulated typical SVA plasma concentration profile for the CC genotype was then compared with the observed data to assess the degree of agreement.

Finally, conditionally on the success of the second aim, the last step was to investigate the effect of the CC genotype not solely on the concentrations in plasma but also in the clinically relevant liver and muscle tissues where data were not available. The model-predicted change in the SVA exposure in these tissues between the wild type (TT) and the variant (CC) genotype was calculated. In addition, the effect of this genotype on the ratio between the SVA unbound liver tissue concentrations and SVA unbound liver plasma concentrations (a dynamic representation of the SVA $KPuu_{liver}$) was also investigated.

Effect of Clinically Important DDIs on SV and SVA Disposition

The effect of a range of different CYP3A inhibitors on SV/SVA disposition was selected to be evaluated in the current work, namely itraconazole (ITZ) 200 mg, erythromycin (ERY) 500 mg, clarithromycin (CLR) 500 mg and diltiazem (DTZ) 120 mg. The selection was based firstly on the fact that the

interaction between these CYP3A inhibitors and simvastatin has been clinically studied and the degree of interaction is clinically important (associated with specific recommendations in simvastatin package label). Secondly, this list includes DDIs with various degrees of complexity ranging from competitive to mechanism-based inhibition and to DDIs where both the parent compound and its metabolite have CYP3A inhibition capability. Therefore, the model and its assumptions were tested over a number of different conditions which were not part of the model development set.

The general workflow to predict the effect of these DDIs on SV/SVA disposition is briefly described below. Firstly concentration profiles of inhibitors of interest were generated with Simcyp v13 using the minimal PBPK model [23]. The standard assumption associated with this model when applied for DDI prediction is that the simulated unbound concentrations in portal vein and liver reflect those at the enzyme site in the small intestinal wall and liver respectively [23]. Subsequently these generated concentration profiles were used after interpolation (with the "interp1" function in Matlab R2012a) as forcing functions for the interaction in the small intestinal wall and liver tissue compartments of the developed SV/SVA mechanistic model. The differential equations in these model compartments were modified accordingly in order to describe the DDI mechanism in the presence of the inhibitor(s) and the consequent decrease in SV/SVA CYP3A metabolism. The mathematical relationships used to model the interaction, the relevant input parameters such as inhibition constants and all the other relevant information for each of the evaluated DDIs are summarised in Supplement 6. Model predictions were performed using the typical parameters of the developed model and the mean population characteristics (*e.g.* weight) in each of the four investigated DDI studies. For each of these interactions, the model-predicted change in SV/SVA plasma Cmax and AUC was calculated and compared to the observed values from reported clinical DDI studies. The interaction effects on the liver and muscle SV/SVA concentrations were also investigated.

RESULTS

SV/SVA Physiological Population PK Model

The parameter estimation process together with a covariance step were completed successfully for the developed population model with the FOCE-I method. The estimation and covariance steps were completed in 18.7 and 42.2 h, respectively. The informative prior B, (Supplement 4 section 2.2) was selected to describe the prior knowledge regarding SV permeability from the lumen to the small intestinal wall in the final model as it increased model stability. The parameter estimates of the final population pharmacokinetic model are reported in Table III. Relative standard errors (RSE) were less than 25 and 50% for all the estimated fixed and random effects respectively. As was expected, the RSE with respect to model parameters with very strong prior information are small, as the parameter estimates in such situations are dictated from the prior knowledge.

The NONMEM-obtained MAP point estimates of the population model parameters which were supported by informative priors were plotted on top of the distributions representing the available prior knowledge (prior uncertainty in a population model parameter), in order to visualise the degree that these estimates were updated from the priors (Fig. 2). It was observed that many of the structural model parameters were indeed informed from the available data updating prior knowledge (Fig. 2). In particular, this was evident for the SV CYP3A intrinsic clearance ($CLint_{CYP3A,vitro}$), the SV permeability to the small intestinal wall (P_{eff}) and the SV/SVA partition coefficients (*e.g.*, $KPu_{T:P,m}$). In contrast, for model parameters which cannot be substantially informed from the plasma data and for which strong prior information was available, the MAP estimates shrunk towards the prior (Fig. 2). Specific examples are the parameters representing SV to SVA hydrolysis in muscle ($k_{hydr,buff}$) and liver tissue ($k_{hydr,S9}$) and the SVA to SV lactonisation in liver tissue ($CLint_{gluc,vitro}$). In addition, the estimates for the inter-individual variability variance terms associated with gastric (η_{GRT}) and small intestinal (η_{SIRT}) residence times were governed (Fig. 2) by the provided strong prior knowledge (Supplement 3 section 2). The population model parameters for which completely uninformative priors were provided (Table II) were adequately informed from the available data evidenced by the associated low RSE (*e.g.*, CLu_{act}, Table III).

The parameter estimation process with the parallelised IMPMAP method was also completed successfully. All the associated parameter estimates and a complete comparison with the FOCE-I estimates are provided in Supplement 2 (section 2). Overall, the parameter estimates from the FOCE-I and IMPMAP methods were very similar with the latter method showing substantial improvements in convergence time.

The first step towards the validation of this mechanistic population model was to assess the physiological / mechanistic plausibility of the parameter estimates. None of these parameter estimates could be regarded as physiologically non-realistic (see Discussion for further comments). In order to aid the assessment of the inter-conversion parameter estimates, the SV-SVA inter-conversion rate constants applied in the different model compartments were calculated and reported in Supplement 7 (Table S7.1). The magnitude of SV to SVA hydrolysis rate constants in the different model

Table III Parameter Estimates of the Final SV/SVA Population Pharmacokinetic Model

Model parameter	NONMEM estimate (RSE%) [a]	Bootstrap estimate [b] (RSE%) [a]
Structural model [c]		
P_{eff} (cm/h)	1.2738 (20.00)	1.3301 (21.31)
$CLint_{CYP3A,vitro}$ (μL/min/pmol CYP3A)	13.874 (7.97)	14.208 (8.61)
$KPu_{T:P,m}$	4315.6 (23.72)	4362.8 (21.12)
$KP_{T:B,rob}$	19.106 (7.34)	18.716 (7.98)
$KPu_{T:P,lt}$	2892.9 (18.45)	3033.6 (15.68)
$CLint'_{CYP3A,vitro}$ (mL/min/mg of MP)	0.0513 (12.55)	0.0504 (18.41)
$KPu'_{T:P,m}$	1.3965 (18.66)	1.4562 (21.90)
$KP'_{T:B,rob}$	0.9501 (17.33)	1.0476 (24.51)
CLu_{act} (L/h)	8266.8 (21.23)	8001.1 (18.70)
$k_{hydr,pl}$ (h^{-1})	0.1300 (8.82)	0.1264 (7.77)
$k_{hydr,buff}$ (h^{-1})	0.0260 (0.003)	0.0260 (0.005)
$k_{hydr,S9}$ (h^{-1})	0.0639 (0.37)	0.0640 (0.36)
$CLint_{gluc,vitro}$ (μL/min/mg of MP)	0.3701 (0.58)	0.3703 (1.79)
$k_{hydr,hybrid}$ (h^{-1})	2.7732 (13.87)	2.7457 (13.24)
Inter-individual variability (%CV) [d]		
GRT	37.00 (0.001)	37.00 (0.001)
SIRT	41.96 (0.001)	41.96 (0.001)
P_{eff}	118.68 (34.81)	118.47 (29.45)
$CLint_{CYP3A,vitro}$	38.32 (41.53)	36.51 (41.12)
$KP_{T:B,rob}$	36.49 (25.84)	35.19 (25.53)
$CLint'_{CYP3A,vitro}$	38.62 (49.71)	38.30 (140.53)
$KP'_{T:B,rob}$	69.81 (41.56)	61.00 (64.23)
CLu_{act}	70.77 (39.16)	71.87 (54.48)
$k_{hydr,hybrid}$	63.75 (32.84)	59.86 (39.48)
Residual variability [e]		
eps_{SV}	0.272 (15.15)	0.268 (15.38)
eps_{SVA}	0.117 (14.96)	0.115 (16.57)

When any of the above parameters is relevant to both SV and SVA, the parameter abbreviation referring to SVA is followed by a prime. Abbreviations are exactly as listed in Table II. Additional abbreviations used here are: MP: microsomal protein; GRT and SIRT: gastric and small intestinal respectively residence time

[a] Relative standard errors (RSEs) were calculated as: (standard error/estimate) · 100. For the structural model parameters, normal/log-normal reverse algebra (Supplement 4 section 1) was utilised to obtain the RSEs in the domain of the reported original parameter instead of the log-transformed domain

[b] Estimates are reported as the median from the bootstrap samples ($n = 104$)

[c] Typical population estimates for the structural model parameters were derived after natural exponentiation of the estimated log-transformed parameter

[d] Coefficient of variation (% CV) is calculated as: $\sqrt{(e^{\omega^2}-1)} \cdot 100$. For GRT and SIRT which have been assumed to follow a logit-normal generalisation, the expected value and variance of the distribution were computed by numerical integration in order to calculate the reported CV

[e] Residual variability is reported as variance terms (an additive error model was applied on the log-transformed data). eps_{SV} and eps_{SVA} correspond to the residual error variance associated with SV and SVA plasma concentrations respectively

compartments was: liver tissue > > systemic blood, liver vascular compartment > small intestinal wall, rest of body compartment > muscle. The lactonisation rate constant in the liver tissue was calculated to be 1.1% of the hydrolysis rate constant in the same tissue.

Subsequently, the next step was to assess the robustness of parameter estimates and the ability of the model to adequately describe the observed (fitted) plasma concentrations and their variability. From the 114 samples of the bootstrapping procedure, a subset ($n = 104$) with successfully converged model fits was used to obtain descriptive statistics regarding the parameter estimates. The median time for convergence across these bootstrap samples was 29.5 h. The parameter estimates and relative standard errors obtained from the bootstrapping procedure are also reported in Table III. Although the bootstrap sample size is relatively small (due to the computational burden of the model), very good agreement was observed between NONMEM estimates/standard errors from the original dataset and the bootstrapping procedure (Table III), providing additional evidence regarding model stability and absence of bias. The only exception to this agreement (Table III) was the standard error of the inter-individual variability estimate of the SVA CYP3A-mediated intrinsic clearance ($CLint'_{CYP3A,vitro}$). The difficulty associated with the estimation of this random effect term is understandable when considering that due to the permeability-limited hepatic distribution of SVA, the observed population variability in plasma concentrations is affected to a much higher degree by the population variability in active hepatic uptake clearance rather than the variability in intrinsic metabolic clearance [24] (see Supplement 7 section 1 for further discussion).

Typical goodness of fit plots with respect to the developed population model are presented in Supplement 7 and specifically Figures S7.1 and S7.2 for SV and SVA respectively. None of these plots indicated any misspecifications in the structural and statistical model. A visual predictive check (VPC) of the developed physiological population pharmacokinetic model stratified by study is presented in Fig. 3. It can be observed that the model has a very good predictive performance as it adequately reflects the data and their variability for both SV and SVA across both studies.

The results of the external model validation are presented in Supplement 7 (Figure S7.3) in the form of a visual predictive check of the model with regard to the non-fitted independent dataset (as described in Supplement 5 section 2). Although a small degree of bias can be observed (mainly for SVA), the developed model shows a very good performance in terms of prediction of both average concentration profiles and population variability. This is of significant importance when considering that the data used for external validation were

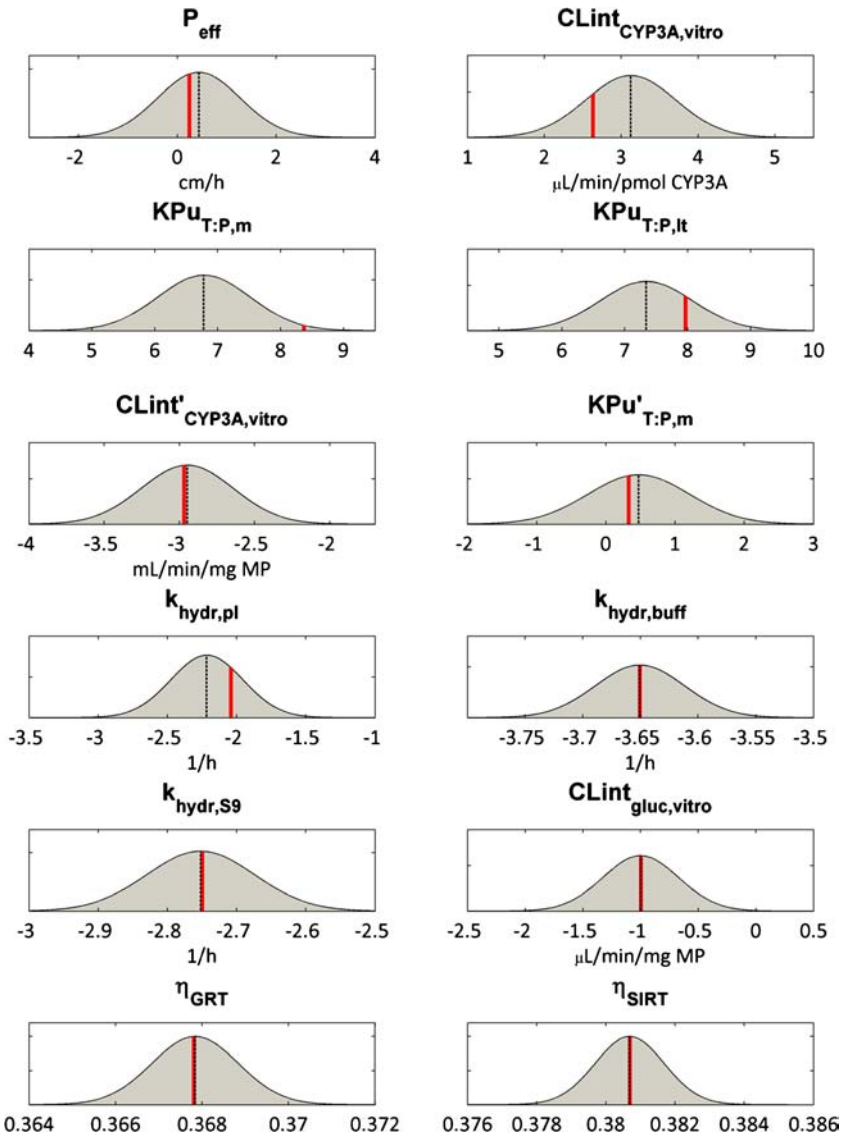

Fig. 2 MAP point estimates (*red lines*) of the population model parameters which were supported by informative priors, plotted on top of the distributions (*grey areas*) representing the available prior knowledge (uncertainty in a population model parameter). The prior modes are represented with black dotted lines. All subplots are referring to the natural log of structural model parameters apart the two bottom subplots that are referring to the inter-individual variability variance terms (η) associated with gastric (η_{GRT}) and small intestinal residence time (η_{SIRT}). When any of the above parameters is relevant to both SV and SVA, the parameter abbreviation referring to SVA is followed by a prime. Abbreviations are exactly as listed in Table II.

from a completely independent study [22] with a different study design, different analytical methodology and different population characteristics compared to the studies used for model development (discussed in Supplement 5 section 2). Therefore, additional confidence was provided that the parameter estimates of the developed model are not specific only for the population used for model development and use of the model outside the studied population and experimental conditions is justifiable.

As explained in the methods section, the developed model was used to predict typical concentration profiles for both SV and SVA not only in plasma but in the other clinically relevant tissues which are the liver (efficacy) and the muscle (toxicity). These typical concentration profiles are presented in Supplement 7 (Figure S7.4).

SV bioavailability (F) for a typical individual was predicted to be 4.21%. The constituent components of F for a typical individual were 0.6195, 0.389 and 0.1747 for F_a, F_g and F_h respectively. Population variability for bioavailability and its constituent components was also assessed. The 90% population prediction intervals for F, F_a, F_g and F_h were (1.11, 9.98%), (0.263, 0.852), (0.246, 0.556) and (0.089, 0.351) respectively. It should be clearly noted that these parameters and their population variability are not direct outcome of parameter estimation but are calculated with a simulation-based procedure that takes advantage of the mechanistic model structure (Supplement 5 section 3). The magnitude of the acid-lactone back-conversion (recycling) process was determined to be minor, as in a typical individual the recycling fraction (F_{REC}) parameter was calculated to be 0.91%. Population variability in F_{REC} was also assessed and the 90% population prediction intervals were (0.48, 1.63%).

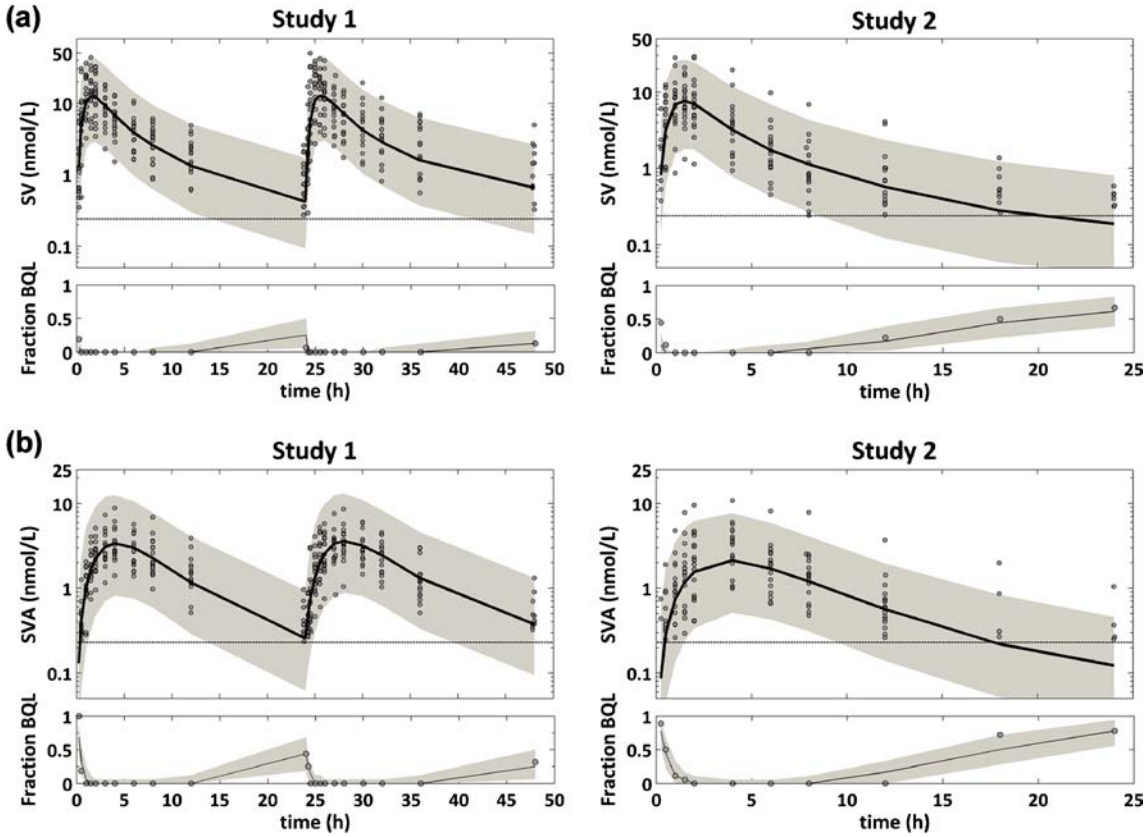

Fig. 3 Visual predictive check (VPC) of the developed population model stratified by study for both SV (**a**) and SVA (**b**) plasma concentrations. In the upper panels, *closed circles* represent the observed plasma concentrations; *highlighted with grey* are the areas between the 5th and 95th percentiles of model simulations, whereas the *black solid line* represents the median; the *horizontal dashed black line* represents the limit of quantification. In the lower (smaller) panels, *grey areas* represent the simulation-based 95% confidence intervals for the fraction of model simulated samples below the limit of quantification (BQL) at each time point, whereas the *black solid line* represents the median; the actual observed fraction of BQL samples at each time point are represented with *closed circles*.

Model Applications

Effect of the OATP1B1 c.521 T>C (CC) Genotype on SV and SVA Disposition

The developed model was able to very accurately describe the observed SVA plasma data [18] for the OATP1B1 c.521 T>C homozygous wild type (TT) genotype. A very high degree of agreement was observed between the model-predicted typical profile and the observed SVA concentrations in the TT individuals (Fig. 4b). The CC genotype for this locus was estimated to decrease the SVA *in vivo* active uptake clearance into the hepatocytes (CLu_{act}) by 90.2% (the fractional change was estimated as 0.902 with a standard error of 0.012). With the inclusion of only this covariate effect the developed mechanistic model was able to very adequately describe the observed plasma SVA data for the CC genotype group as well (Fig. 4b).

Taking advantage of the model's mechanistic structure, SV/SVA liver and muscle tissue concentrations were predicted for both the TT and CC genotypes. These concentration profiles are presented in Fig. 4. It can be observed that this polymorphism has no effect on the concentration profiles of the lactone form (SV) in plasma, liver and muscle (Fig. 4a). In contrast, this polymorphism has a substantial effect on the disposition of the acid form (SVA). The SVA plasma and muscle concentrations in individuals with the variant CC genotype are significantly increased compared to the wild-type TT genotype (Fig. 4b). Specifically in both plasma and muscle tissue the SVA exposure obtained from model simulation (AUC_{0-24}) is increased by approximately 171% in the CC variant genotype. However, the SVA concentrations in the site of action (liver) are only slightly affected, as the SVA liver exposure is only decreased by approximately 2% in the CC variant genotype (Fig. 4b). The effect of this genotype on the ratio between the SVA unbound liver tissue concentrations and SVA unbound liver plasma concentrations (a dynamic representation of the SVA $KPuu_{liver}$) is illustrated in Supplement 7 (Figure S7.5). As expected, the equilibrium SVA $KPuu_{liver}$ is much smaller for the CC genotype (3.2 compared to 31.2 for TT) due to the decreased penetration of SVA into the hepatocytes.

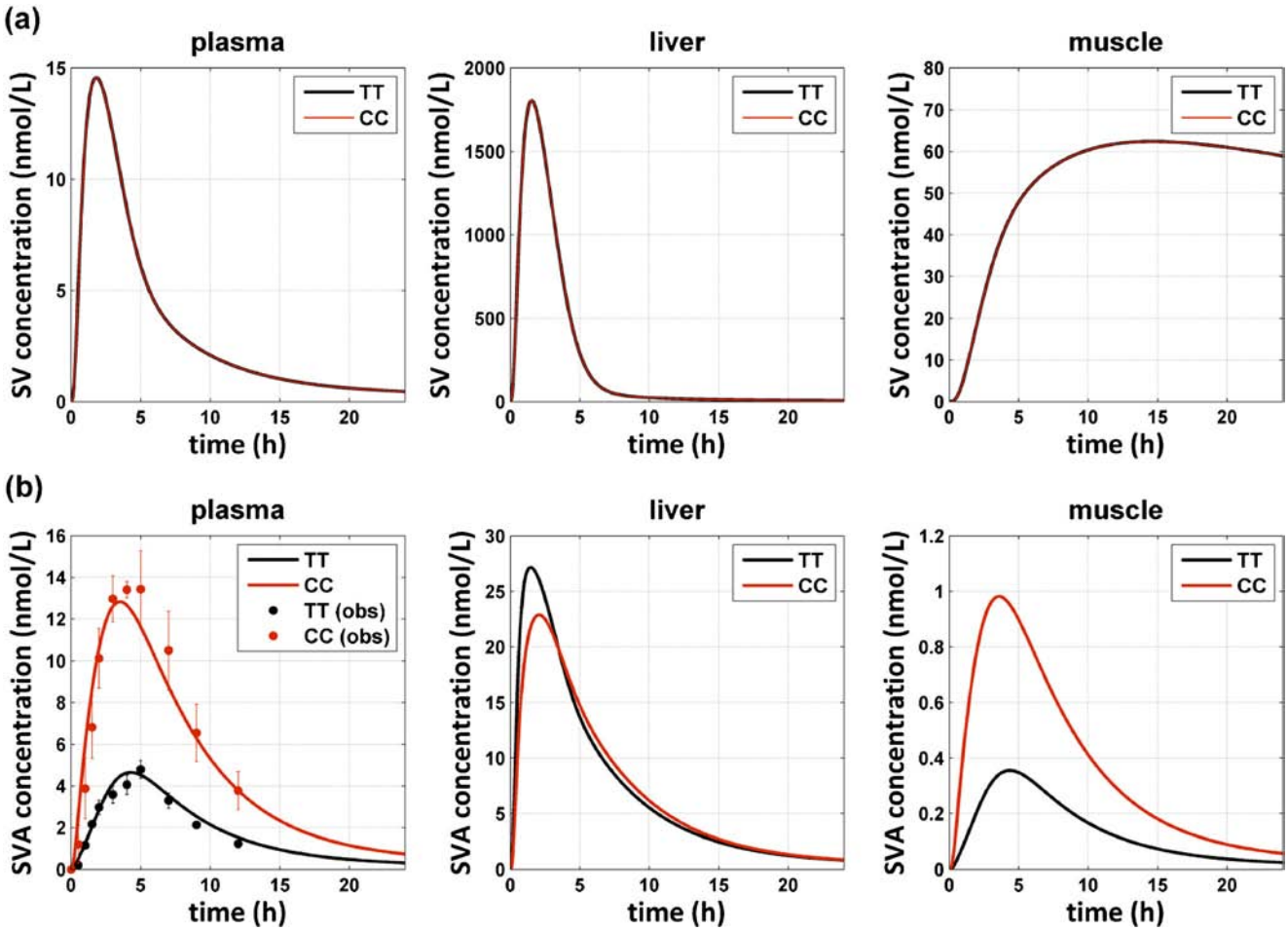

Fig. 4 Simulated typical concentration profiles for both SV (**a**) and SVA (**b**) in plasma, liver tissue and muscle tissue for individuals with the homozygous wild-type TT (*black line*) and homozygous variant CC (red line) OATP1B1 c.521 T > C genotype. In (**a**) the TT and CC simulated concentration profiles are practically identical as the polymorphism does not affect the lactone form (SV). In (**b**) the observed mean ± SE plasma SVA concentrations for individuals with the TT (*black circles*) and CC (*red circles*) genotype from Pasanen *et al*. [18] are also plotted.

Effect of Clinically Important DDIs on SV and SVA Disposition

The developed model successfully predicted the effect of a range of CYP3A inhibitors on the pharmacokinetics of both SV and SVA. All the DDI model predictions are numerically summarised and compared to the observed data from clinical studies in Supplement 7 (Table S7.2). An overview regarding the degree of the model predictions success is presented in Fig. 5. It was observed that the developed model generally predicts the increase in both SV and SVA PK parameters (AUC and Cmax) within 1.5-fold of the observed values (Fig. 5). The only DDI effect that was predicted outside of this range was the effect of ITZ on SV Cmax; however, even this model prediction still lies within two-fold of the observed value. It should be also noted that the reported ITZ interaction effects are related with a degree of uncertainty due to the assay limitations of the clinical DDI study [25]. Among the other investigated DDIs, CLR was the inhibitor for which the model provided the most accurate predictions when compared to the observed data. Specifically, the model predicted an increase in plasma SV AUC and Cmax by 10.02- and 6.49-fold respectively and 11.46- and 8.97-fold increase in SVA AUC and Cmax respectively, following a week of co-administration of 40 mg simvastatin with twice-a-day 500 mg CLR. The agreement with the observed values was excellent as the respective reported values were 9.95, 7.14, 12.17 and 10, respectively [26]. The model-predicted typical SV/SVA concentration profiles not only in plasma but also in liver and muscle tissues for this particular interaction are presented in Fig. 6. The SV/SVA model-predicted typical plasma, liver and muscle concentration profiles for the DDIs with ITZ, ERY and DTZ are provided in Supplement 7 (Figures S7.6, S7.7 and S7.8 respectively). The model predictions with regard to the fold-increase in SV and SVA exposure in plasma, liver and muscle tissue due to the investigated DDIs are summarised in Table IV. For the ERY, CLR and DTZ interactions which have a mechanism-based inactivation component, the model-predicted fraction of active CYP3A

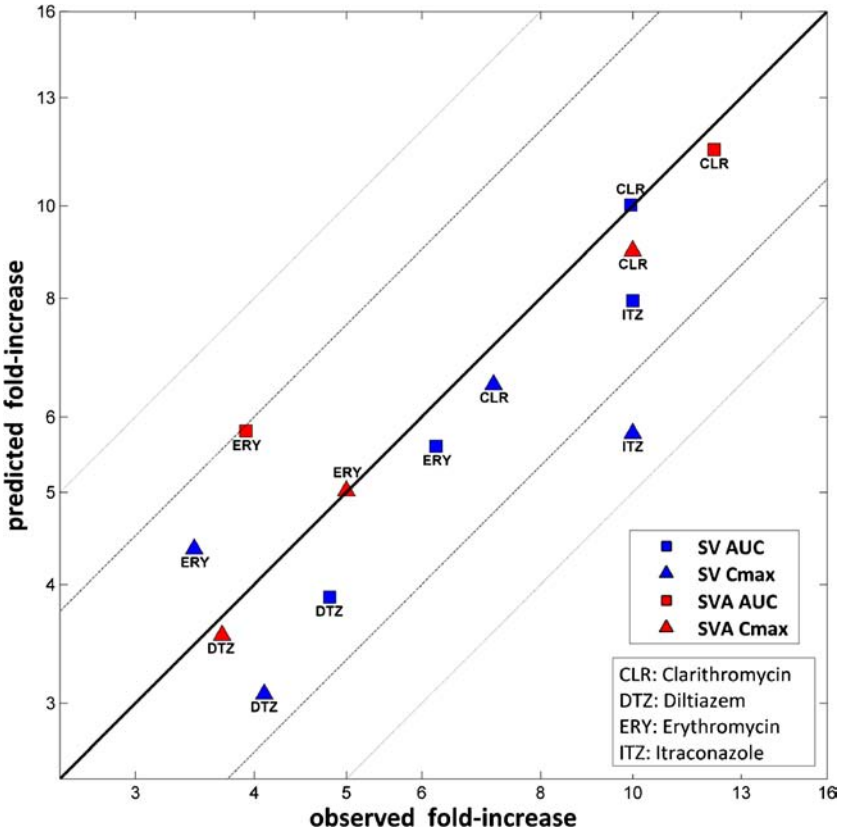

Fig. 5 Overview of the degree of success of model predictions with regard to the investigated DDIs. *Markers coloured in blue and red* represent the effect of the inhibitor on the PK parameters of SV and SVA respectively. *Square and triangular markers* refer to AUC and Cmax respectively. For example, a *blue square marker* refers to the effect of the inhibitor on SV AUC. The name of the inhibitor is specified next to each marker. *Black solid line* represents the line of identity between observed and predicted values; *dashed and dotted lines* represent the 1.5- and 2-fold error intervals respectively. All the exact predicted and observed fold-increase values are reported in Supplement 7 (Table S7.2).

enzyme in the small intestinal wall and liver against time is presented in Supplement 7 (Figures S7.9, S7.10 and S7.11 respectively).

DISCUSSION

SV/SVA Physiological Population PK Model

Besides the widespread use of simvastatin and the clinical burden of muscle toxicity our understanding with regard to the complex SV/SVA pharmacokinetics is still limited. In the current work, a physiologically based population model was developed that mechanistically describes the disposition of both SV and SVA and their inter-conversion in different tissues.

As the parameters of the developed model are mechanistic in nature and represent actual physiological processes, they were assessed in terms of physiological plausibility. In the current model, most of the parameters are provided with informative priors derived from *in vitro/ in silico* experiments and physiology knowledge and therefore this approach in a way guards against the probability that some of the parameters are estimated outside their physiological range. As it can be observed in Fig. 2 the model parameters provided with informative priors converged to estimates which are within the prior knowledge range. However, specific attention should be given with regard to the physiological plausibility of model parameters which either converged to a region not particularly well covered by the prior distribution (SV muscle tissue to unbound plasma partition coefficient, $KPu_{T:P,m}$) or those that due to lack of information were not supported at all by informative priors (*e.g.* SVA active uptake clearance into the hepatocytes, CLu_{act}). The arguments supporting the physiological plausibility of the above two parameter estimates are in particular discussed in Supplement 7 (section 2).

The estimates of the "rest of body" partition coefficients cannot be interpreted *per se* as they refer to an empirical peripheral space (see Supplement 1). However, the product of the estimated partition coefficient and the known physiological volume of the "rest of body" compartment (≈33 L) can be indicative of the extent of the compound's distribution in

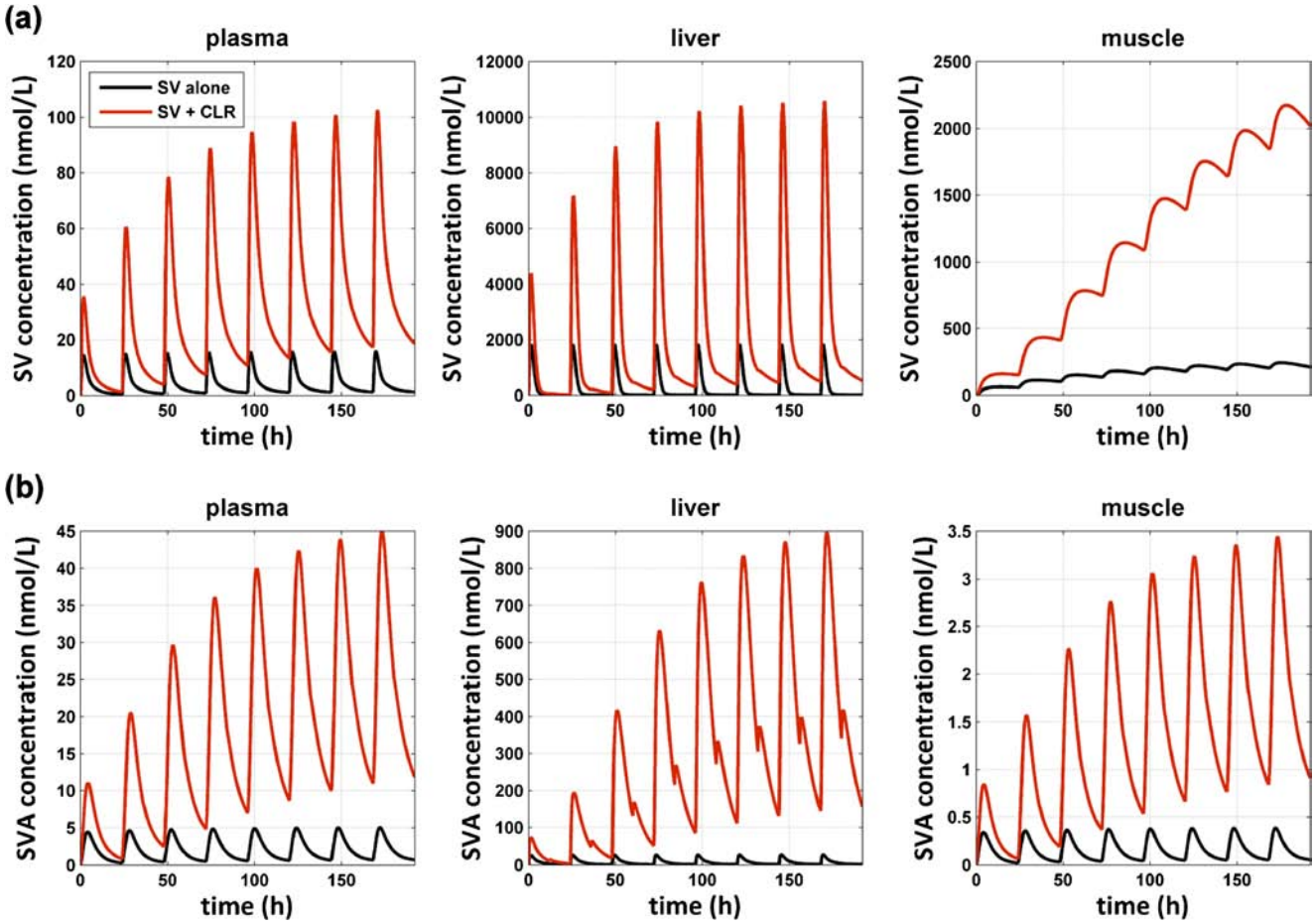

Fig. 6 Model simulated typical concentration profiles for both SV (**a**) and SVA (**b**), in plasma, liver tissue and muscle tissue, after multiple doses of 40 mg simvastatin administered with (*red line*) or without (*black line*) clarithromycin (CLR) 500 mg twice-a-day. The small irregularities (secondary peaks) observed in the liver SVA concentrations occur at times that CLR doses were administered and are a consequence of SV to SVA hydrolysis.

this empirical peripheral space. The tissue to plasma partition coefficients for the rest of the body compartment were estimated 10.9 and 0.53 for SV and SVA respectively. Similarly, the muscle tissue to plasma partition coefficients were estimated as 57.8 and 0.08 for SV and SVA respectively. These results are in agreement with the SV and SVA physicochemical properties. Specifically, they indicate that the highly lipophilic lactone form (SV) is extensively distributed into several tissues, in contrast to the much more hydrophilic acid form (SVA) for which distribution is mainly limited to tissues with active uptake capability (liver). Apart from the increased mechanistic understanding of the SVA disposition, the results of the current work also highlight that the assumption of equal volumes of distribution of the metabolite (SVA) and the parent drug (SV) that has been used before in SV/SVA population models [27] (to resolve identifiability issues) is unjustifiable.

The developed model also provides further insight regarding the complex inter-conversion process between SV and SVA in the different tissues. After calculation of the SV-SVA inter-conversion rate constants applied in the different model compartments (Supplement 7, Table S7.1) it is obvious that the compartment that has the highest capability of SV to SVA hydrolysis is by far liver tissue. This is in agreement with previous experimental work that identified the liver as the tissue having the most abundant expression of carboxylesterases in humans [28] and together with previous knowledge that the liver is the tissue that SV is mainly bioactivated to SVA [1]. In addition, the developed model also accounted for the SV to SVA hydrolysis in plasma and the small intestinal wall. Although the latter is acknowledged in the literature [29,30], it has never been quantified prior to this work. Our estimate regarding the SV to SVA hydrolysis in the small intestinal wall can be considered as mechanistically sound. This is based on the fact that the associated hydrolysis rate constant (Supplement 7, Table S7.1) is higher than the hydrolysis rate constant observed *in vitro* in a pH 7.4 buffer (where hydrolysis is mediated only chemically) but much smaller than the hydrolysis rate in the liver tissue (the tissue with the most abundant expression of carboxylesterases). It should be also noted that although the capability of the small intestinal wall for SV to SVA hydrolysis is much smaller compared to the liver, it is a process that should not be

Table IV Model predicted DDI effect on SV/SVA plasma, liver and muscle tissue exposure

	Plasma	Liver	Muscle
Itraconazole (ITZ)			
SV	7.95	8.14	7.40
SVA	8.53	33.18	8.53
Erythromycin (ERY)			
SV	5.59	5.70	5.28
SVA	5.80	16.94	5.80
Clarithromycin (CLR)			
SV	10.02	10.46	9.12
SVA	11.46	61.93	11.46
Diltiazem (DTZ)			
SV	3.88	3.93	3.72
SVA	3.96	9.20	3.96

The values reported above represent the fold-increase in SV and SVA exposure (AUC) in plasma, liver and muscle tissue caused by each of the investigated DDIs. Plasma, liver and muscle tissue exposures were predicted by simulation with the developed model until 24 h post-SV-dose. For all inhibitors the SV dose was 40 mg apart from DTZ where a 20 mg dose was given. For CLR where multiple SV doses where given, the reported fold-increase in exposure refer to the last dosing interval

neglected as the amount of SV available for hydrolysis in this tissue is substantial. Consequently, the plasma concentrations of SVA are particularly sensitive to this process. Finally, the presented model also mechanistically described the back-conversion (lactonisation) of SVA to SV. The lactonisation rate constant in the liver tissue was much smaller than the hydrolysis rate constant in the same tissue (Supplement 7, Table S7.1), indicating that the formation of SVA is significantly favoured inside the liver. In addition, the magnitude of the back-conversion (recycling) process was determined to be minor, as in a typical individual the recycling fraction (F_{REC}) parameter was calculated to be 0.91%. These results are in agreement with a previous *in vivo* study (dogs) which also suggested a minor involvement of SVA back-conversion and a fraction recycled of <1% [4]. However, the incorporation of this process in the model is important due to the fact that the liver concentrations of SVA (related to efficacy) can be particularly sensitive to perturbations of the components of this inter-conversion process (from sensitivity analysis, data not shown).

The mechanistic structure of the model allowed also the investigation of simvastatin bioavailability (F) and its constituent components (F_a, F_g and F_h). The bioavailability of simvastatin was predicted for a typical individual to be 4.21%, which is in agreement with the current knowledge that less than 5% of a simvastatin dose reaches the circulation system in humans [1]. This provides additional confidence that the model adequately captures the first pass metabolism of SV.

Overall, the developed model offered a very accurate description of the observed data and their variability illustrating the suitability of the nonlinear mixed effects modelling approach to analyse population data even with such complex PBPK models. The long computational times represent one of the main obstacles during the development of these population models. However, we illustrated in this work that even this hurdle can be further diminished with the application of alternative estimation methods (*e.g.* IMPMAP, see Supplement 2) which can be fast and efficiently parallelisable for such complex differential equation models [31].

Before continuing to the discussion of the model applications, a particular model assumption with regard to the disposition of SVA has to be highlighted. It has been assumed in this work that the distribution of SVA in the muscle is perfusion-limited and not transporter mediated. There is some evidence suggesting that the OATP2B1 transporter may be responsible for the active uptake of other statins (atorvastatin and rosuvastatin) into human skeletal muscle [32]. However, despite the substantial research associated with simvastatin-induced myopathy, to our knowledge, there is no evidence with regard to the specific mechanism by which SVA permeates into human muscle tissue. Therefore, as the contribution of active uptake of SVA in muscle tissue remains unclear and in the absence of observed SVA muscle tissue concentrations, the model assumption of perfusion-limited distribution derives from lack of information. However, as this model assumption can affect the predicted SVA concentrations in the muscle tissue, it should be clearly underlined. Hopefully, future research will shed some light into this important aspect of SVA disposition.

Model Applications

The developed model was used to extrapolate beyond the studied population and experimental conditions. The scenarios investigated here (OATP1B1 polymorphism and CYP3A inhibition) are of substantial clinical interest as they both have been associated with the development of simvastatin-induced myopathy. In addition, taking advantage of the physiological structure of the model we were able to determine the effects of these conditions not solely on the plasma concentrations of SV and SVA, but also on the concentrations in the sites relevant to the efficacy (liver) and toxicity (muscle) of the drug.

Effect of the OATP1B1 c.521 T>C (CC) Genotype on SV and SVA Disposition

The SV/SVA model was able to successfully describe the observed plasma data from a previous pharmacogenetic study regarding the OATP1B1 (*SLCO1B1*) c.521 T>C (rs4149056) polymorphism (Fig. 4). The application of a single covariate term in the model parameter where this polymorphic effect is

manifested, the SVA active uptake clearance (CLu_{act}), was enough to adequately capture the effects of the homozygous variant CC genotype on the SVA plasma concentrations. This provided further evidence that the model structure, assumptions and parameters are mechanistically robust. The ability to apply this covariate directly on the parameter where it mechanistically lies is a significant advantage of this physiological model over previous population models with empirical structures, where the effect of the OATP1B1 genotype had to be applied to the surrogate clearance and volume terms [9]. In the current work we identified that the SVA *in vivo* active uptake clearance into the hepatocytes (CLu_{act}) in individuals with the homozygous variant CC genotype is approximately 10% of the value assigned to the homozygous wild type subjects. This is in agreement with the current literature as taking in to account previous findings of both *in vitro* and *in vivo* approaches [33–36], it was expected that this estimate should lie within the range of 0–35%.

It was observed in our simulations that this OATP1B1 polymorphism does not affect the concentration profiles of the lactone form (SV), (Fig. 4a). This is in agreement with the findings of a previous pharmacogenetic study [18] and it is justifiable based on the fact that the highly lipophilic lactone form can readily penetrate the hepatocytes through passive diffusion and therefore does not depend on OATP1B1 activity. In contrast, the concentration profiles of the much more hydrophilic acid form (SVA) were substantially affected by this polymorphism (Fig. 4b). It should be noted that the magnitude of the back-conversion process from SVA to SV is so small (discussed above) that these changes in SVA disposition cannot propagate back to the lactone concentrations. Our results indicated that the homozygous variant CC genotype for the OATP1B1 polymorphism significantly increases SVA exposure in plasma and muscle tissue (Fig. 4b). More specifically the degree of this increase in plasma and muscle is comparable. These model predictions are in agreement with the clinically observed effects of this polymorphism which has been robustly and repeatedly associated with simvastatin induced myopathy [37]. However, although our results suggest that the polymorphism effect on SVA plasma exposure very well reflects the situation in muscle tissue, this is not the case with regard to the effect at the drug's site of action (liver). Specifically, it was observed that in individuals having the homozygous variant CC genotype for this polymorphism, the SVA liver exposure is only marginally affected (decreased approximately by only 2%), (Fig. 4b). This model prediction is in agreement with the clinically observed data which suggest that this OATP1B1 polymorphism has not been associated with any clinically significant alterations in the cholesterol lowering efficacy of simvastatin [8]. Specifically, among 16,664 genotyped participants of the Heart Protection Study, the reduction in the LDL cholesterol level was only 2.56% smaller in the homozygous variant CC subjects [37]. Hence, what is illustrated here is an interesting case where the polymorphism effect on the concentrations at the drug's site of action diverges from the effect on plasma concentrations. Consequently it is inappropriate to link plasma concentration to the efficacy of the drug which has to be related to the local tissue concentrations. The model predictions that illustrate that SVA liver exposure is not sensitive to changes in active uptake clearance are also in agreement with previous modelling work with other OATP1B1 substrates, pravastatin [38] and rosuvastatin [36]. As it has been repeatedly discussed and illustrated in the literature [38,39], this effect is due to the fact that for compounds which permeate the hepatocytes predominately by active uptake and their elimination is primarily hepatic, their liver exposure is determined by either the metabolic and/or biliary clearance rather than active uptake (see also Supplement 8 for an analytical justification of this concept). However, to the best of our knowledge this is the first time that the above concept has been mechanistically illustrated in the case of the active metabolite of simvastatin, SVA. In contrast to pravastatin and rosuvastatin which are administered in the active open acid form, in the case of simvastatin the additional process of SVA formation inside the liver tissue has to be considered adding further complexity.

Effect of Clinically Important DDIs on SV and SVA Disposition

The second model application investigated in this work was the prediction of the effects of a range of different CYP3A inhibitors on the pharmacokinetics of both SV and SVA. The developed model very adequately predicted the reported increase in SV and SVA plasma AUC and Cmax associated with these clinically important DDIs (Fig. 5). It is important to note that these predictions were performed without the use of any clinical interaction data to optimise model parameters associated with the inhibition. The ability of the developed model to successfully predict the interaction effects not solely on SV but also on SVA is of particular importance. As SVA is the active form, prediction of the interaction effects on SVA concentrations is crucial in order to investigate the effects on both the toxicity and therapeutic efficacy of the drug and suggest possible dose adjustments. In addition, the ability of the current model to successfully predict the interaction effects on both SV and SVA forms, serves as an additional model validation illustrating that the lactone to acid conversion in the sites of interaction (small intestinal wall and liver) is adequately described. Although physiologically-based models for the disposition of simvastatin have been published before [35,40], to our knowledge this is the first time where such a model has been successfully validated for its ability to simultaneously predict interaction effects on both SV and SVA forms.

The effects of these clinically important DDIs were also investigated with regard to the liver and muscle SV/SVA concentrations. All the evaluated DDIs were predicted to

cause a substantial increase in the muscle exposures of both SV and SVA (Fig. 6 and Supplement 7: Figures S7.6–S7.8). Specifically, the fold-increase in SV and SVA muscle exposures ranged from 3.72 and 3.96 respectively for the diltiazem DDI, up to 9.12 and 11.46 for the clarithromycin DDI (Table IV). These substantial model-predicted increases in SV/SVA muscle exposure are in agreement with the clinically reported fatal cases of rhabdomyolysis related to such DDIs [41]. They are also in line with the current recommendations which state that co-administration of simvastatin with clarithromycin, itraconazole and erythromycin is contraindicated, while diltiazem is allowed only in the lowest 10 mg dose [8]. In contrast to the effect of the OATP1B1 polymorphism, the liver exposure of active form (SVA) was predicted to be substantially affected by CYP inhibition. This effect is expected since the liver exposure of such a compound is particularly sensitive to changes in metabolic clearance (as discussed above and in Supplement 8). All the investigated DDIs were predicted to substantially increase the liver exposure of both SV and SVA (Fig. 6, Supplement 7: Figures S7.6–S7.8). Specifically, the fold-increase in SV and SVA liver exposures ranged from 3.93 and 9.20 respectively for the diltiazem DDI, up to 10.46 and 61.93 for the clarithromycin DDI (Table IV). Interestingly, it was observed that the fold-increase in the liver exposure of the active form (SVA) is much more pronounced than the fold-increase in the liver exposure of the lactone (SV) for all the evaluated DDIs. This is justifiable as due to the inhibition of the CYP3A metabolism of SV much more drug is available locally inside the liver to be converted through hydrolysis to the active form (SVA), the CYP3A metabolism of which is also inhibited. This leads to a substantial increase in the local liver concentrations of SVA, which due to its physicochemical properties and low passive diffusion clearance is "trapped" in the hepatocytes. The model-predicted substantial increase in the liver exposure of the active SVA form due to CYP inhibition is in agreement with clinical findings demonstrating that the cholesterol reduction efficacy of simvastatin is significantly enhanced when co-administrated with diltiazem [42].

Dose Reduction Considerations

Overall, from the investigated conditions and the model predictions, it can be concluded that a simvastatin dose reduction in the case of co-administration with a CYP3A inhibitor can decrease the risk of muscle toxicity, while patients are achieving the recommended cholesterol reduction. This is because the decreased SVA liver exposure due to the dose reduction can be counterbalanced with the effect of the DDI (increase in the SVA liver exposure). On the other hand a dose reduction in the case of decreased OATP1B1 uptake clearance (due to polymorphism or inhibition) can decrease the risk of muscle toxicity, but patients might receive a sub-therapeutic dose (as SVA liver exposure is unaffected by the decrease in active uptake clearance). However, large scale clinical data are needed to further investigate and validate these model-derived conclusions.

Further Comments Regarding the Applied Integrated Population PBPK Approach

Parameter estimation in complex PBPK models is increasingly performed in the last few years due to the advances in computational power and the development of specialised modelling and simulation platforms. For this reason, we recently published a paper specifically focused on the discussion of best practices and methodological issues related to parameter estimation in PBPK models [10]. The current work aims to illustrate such a process in practice and provide an example of an integrated population PBPK approach to analyse clinical data. We have previously highlighted that such an approach combining physiologically-based with nonlinear mixed effects modelling and parameter estimation techniques can provide mechanistically sound models at the population level [10]. Some additional advantages of this approach have to be underlined. Firstly, the physiological structure of these models, allows extrapolation outside the studied population and experimental conditions. This was specifically illustrated in this work with the development of a population mechanistic SV/SVA model using data from clinical studies, which was subsequently used to successfully extrapolate and perform predictions outside the studied conditions (*e.g.* CYP3A inhibition). Secondly, as such mechanistic models can provide tissue concentration predictions, the efficacy and toxicity of a drug do not need to be linked to the surrogate plasma concentrations. This was particularly illustrated in this work by performing predictions for the effects of clinically important conditions (OATP1B1 polymorphism, CYP inhibition) not only on SV/SVA plasma but also on liver and muscle concentrations. The model-predicted effects on the local tissue concentrations were in agreement with the clinically observed cholesterol lowering effects and toxicity outcomes of these conditions. Finally, such an approach can inform and guide the design of prospective clinical DDI and/or pharmacogenetic studies even in the first stages of drug development when *in vivo* data are limited. Power calculation prior to such studies is based on an educated guess on the magnitude of the clinical effect and the associated population variability [24]. Population mechanistic models can take advantage of their physiological structure and their ability to extrapolate to provide predictions for the former (*e.g.*, using *in vitro* data); and their stochastic level to provide predictions for the latter. This concept has been specifically highlighted in one of our recent publications where power calculations were performed to guide prospective DDI and pharamacogenetic studies with regard to repaglinide pharmacokinetics [24].

Crucial for the development of population PBPK models is the concept of prior information. The advantages of utilising prior knowledge in the PBPK modelling framework are numerous and have been described elsewhere [10,11]. The most important is that it allows knowledge from several sources (*e.g. in vitro* experiments) to be integrated with the analysed clinical data, supporting parameter identifiability in these complex models. Prior information is typically incorporated in hierarchical population models through Markov chain Monte Carlo (MCMC) Bayesian estimation [43]. Compared to a typical MCMC Bayesian analysis, the maximum a posteriori method used in the current work (see Methods) to incorporate prior information has the inherent disadvantage that it produces point parameter estimates rather than posterior distributions. However, this method retains all the advantages deriving from the use of prior information while also offering stability and significant reductions in the computation time that would have been required for a MCMC Bayesian analysis [13]. This is of particular importance as besides the rapid advances in computer science, computation times still represent a significant burden during the development of such complex models. It should be also noted that in the current work the available prior knowledge with regard to drug-related model parameters derives solely from *in vitro* experiments and *in silico* predictions and not from any previous model fittings of clinical data. This incorporates an additional limitation as some model parameters (especially the random effect inter-individual variability terms) are completely unknown and were provided with non-informative priors. Therefore, it is expected that a MCMC Bayesian analysis in such a complex model might need very long run times or face difficulties to achieve stable MCMC chains and accomplish convergence with regard to these parameters [31,44], especially as only plasma concentrations are observed. On the other hand the maximum a posteriori method used in this work displayed remarkable stability for such a complex model, did not face any convergence issues and was able to precisely estimate even the model parameters for which informative priors were not provided. However, we should clearly state that a formal MCMC Bayesian analysis should be preferable when it is possible, due to the significant advantages deriving from having the complete posterior distribution [45].

We suggest future application of the developed population model to SV/SVA clinical data to be also performed within the same framework. Specifically, we suggest the parameter estimates of the developed model and their associated uncertainty to be used as priors for the analysis of new SV/SVA clinical data either with a maximum a posteriori or with a formal Bayesian MCMC method. Within this framework a continuous flow of information is achieved that produces incremental gains with regard to our knowledge of the studied system/drug. This is particularly illustrated when considering that the presented work can provide a future analysis with strong informative priors with regard to all complex model parameters (both fixed and random effects), while much more limited prior information deriving mostly from *in vitro* / *in silico* experiments was available to us.

The current work is limited by the absence of human liver and muscle tissue concentrations. This is a limitation inherent in the majority of human PBPK models due to the ethical and experimental difficulties to access local tissue concentrations. In the absence of such data the muscle and liver concentration predictions of the current model cannot be quantitatively validated and rely on the underlying modelling assumptions. However, the model predictions were at least qualitatively validated through their agreement with the clinically observed efficacy and toxicity outcomes of the investigated conditions. In addition, the availability of tissue concentrations is not only important for model validation, but within the presented population PBPK framework, tissue data can provide the additional information needed to support identifiability with regard to model parameters that cannot be solely informed from plasma data. The estimation of these parameters was made possible in the current work with the provision of strong informative priors derived from *in vitro* experiments. Nevertheless, it was clearly illustrated that in such a situation the parameter estimates shrink towards the prior (*e.g.*, parameters describing the SV/SVA inter-conversion process at the liver tissue level). On the contrary availability of tissue concentrations would have allowed the *in vitro* knowledge to be updated in the light of the observed tissue data. This is of particular importance as parameter values derived from *in vitro* - *in vivo* extrapolation (IVIVE) may carry a certain degree of inaccuracy and/or imprecision. Given all the above, it is the authors' view that an integrated population PBPK approach as the one presented here, if combined with emerging advanced experimental methods able to determine intracellular concentrations noninvasively [46], can be a powerful tool to further understand drug disposition.

CONCLUSION

In conclusion, the present work provides further insight in the complex pharmacokinetics of SV and its active metabolite, SVA, in humans. The developed model can be of clinical application due to the widespread use of simvastatin and the clinical burden of muscle toxicity [8]. Furthermore, it can be of significant use during drug development for assessing DDI risk of compounds likely to be co-administered with simvastatin. Finally, in the current work the advantages of an integrated population PBPK approach that provides mechanistically sound models at the population level were clearly illustrated.

ACKNOWLEDGMENTS AND DISCLOSURES

N.T. is the recipient of a PhD grant jointly awarded by the University of Manchester and Eli Lilly and Company. A.R-H. is an employee of the University of Manchester and parttime secondee to Simcyp Limited (a Certara Company). Simcyp's research is funded by a consortium of pharma companies. The authors would like to acknowledge the fruitful comments and discussions made by Dr Michael Gertz, Roche and by the members of the Centre for Applied Pharmacokinetic Research at the University of Manchester. The authors would also like to thank Dr Joe Polli for the provision of individual SV and SVA data from Polli *et al.*, 2013 [22].

REFERENCES

1. Mauro VF. Clinical pharmacokinetics and practical applications of simvastatin. Clin Pharmacokinet. 1993;24(3):195–202.
2. Collins R, Armitage J, Parish S, Sleight P, Peto R. MRC/BHF heart protection study of cholesterol lowering with simvastatin in 20,536 high-risk individuals: a randomised placebo-controlled trial. Lancet. 2002;360(9326):7–22.
3. Vickers S, Duncan CA, Chen IW, Rosegay A, Duggan DE. Metabolic disposition studies on simvastatin, a cholesterol-lowering prodrug. Drug Metab Dispos. 1990;18(2):138–45.
4. Prueksaritanont T, Qiu Y, Mu L, Michel K, Brunner J, Richards KM, et al. Interconversion pharmacokinetics of simvastatin and its hydroxy acid in dogs: effects of gemfibrozil. Pharm Res. 2005;22(7): 1101–9.
5. Prueksaritanont T, Subramanian R, Fang X, Ma B, Qiu Y, Lin JH, et al. Glucuronidation of statins in animals and humans: a novel mechanism of statin lactonization. Drug Metab Dispos. 2002;30(5): 505–12.
6. Prueksaritanont T, Gorham LM, Ma B, Liu L, Yu X, Zhao JJ, et al. In vitro metabolism of simvastatin in humans [SBT]identification of metabolizing enzymes and effect of the drug on hepatic P450s. Drug Metab Dispos. 1997;25(10):1191–9.
7. Prueksaritanont T, Ma B, Yu N. The human hepatic metabolism of simvastatin hydroxy acid is mediated primarily by CYP3A, and not CYP2D6. Br J Clin Pharmacol. 2003;56(1):120–4.
8. Ramsey LB, Johnson SG, Caudle KE, Haidar CE, Voora D, Wilke RA, et al. The clinical pharmacogenetics implementation consortium guideline for SLCO1B1 and simvastatin-induced myopathy: 2014 update. Clin Pharmacol Ther. 2014. doi:10.1038/clpt.2014.125 [advance online publication].
9. Tsamandouras N, Dickinson G, Guo Y, Hall S, Rostami-Hodjegan A, Galetin A, et al. Identification of the effect of multiple polymorphisms on the pharmacokinetics of simvastatin and simvastatin acid using a population-modeling approach. Clin Pharmacol Ther. 2014;96(1):90–100.
10. Tsamandouras N, Rostami-Hodjegan A, Aarons L. Combining the "bottom-up" and "top-down" approaches in pharmacokinetic modelling: fitting PBPK models to observed clinical data. Br J Clin Pharmacol. 2013. doi:10.1111/bcp.12234.
11. Leil TA. A Bayesian perspective on estimation of variability and uncertainty in mechanism-based models. CPT: Pharmacosmet Syst Pharmacol. 2014;3:e121.
12. Gisleskog PO, Karlsson MO, Beal SL. Use of prior information to stabilize a population data analysis. J Pharmacokinet Pharmacodyn. 2002;29(5):473–505.
13. Langdon G, Gueorguieva I, Aarons L, Karlsson M. Linking preclinical and clinical whole-body physiologically based pharmacokinetic models with prior distributions in NONMEM. Eur J Clin Pharmacol. 2007;63(5):485–98.
14. Beal SL. Ways to fit a PK model with some data below the quantification limit. J Pharmacokinet Pharmacodyn. 2001;28(5):481–504.
15. Bergstrand M, Karlsson M. Handling data below the limit of quantification in mixed effect models. AAPS J. 2009;11(2):371–80.
16. Boeckman AJ, Sheiner LB, Beal SL. NONMEM users guide - part VIII, help guide. Ellicott City: ICON Development Solutions; 2011.
17. Dokoumetzidis A, Aarons L. Analytical expressions for combining population pharmacokinetic parameters from different studies. J Biopharm Stat. 2008;18(4):662–76.
18. Pasanen MK, Neuvonen M, Neuvonen PJ, Niemi M. SLCO1B1 polymorphism markedly affects the pharmacokinetics of simvastatin acid. Pharmacogenet Genomics. 2006;16(12):873–9.
19. Karlsson MO, Savic RM. Diagnosing model diagnostics. Clin Pharmacol Ther. 2007;82(1):17–20.
20. Zhao P, Rowland M, Huang SM. Best practice in the use of physiologically based pharmacokinetic modeling and simulation to address clinical pharmacology regulatory questions. Clin Pharmacol Ther. 2012;92(1):17–20.
21. Agoram B. Evaluating systems pharmacology models is different from evaluating standard pharmacokinetic-pharmacodynamic models. CPT: Pharmacosmet Syst Pharmacol. 2014;3:e101.
22. Polli JW, Hussey E, Bush M, Generaux G, Smith G, Collins D, et al. Evaluation of drug interactions of GSK1292263 (a GPR119 agonist) with statins: from in vitro data to clinical study design. Xenobiotica. 2013;43(6):498–508.
23. Rowland Yeo K, Jamei M, Yang J, Tucker GT, Rostami-Hodjegan A. Physiologically based mechanistic modelling to predict complex drug-drug interactions involving simultaneous competitive and time-dependent enzyme inhibition by parent compound and its metabolite in both liver and gut—the effect of diltiazem on the time-course of exposure to triazolam. Eur J Pharm Sci. 2010;39(5):298–309.
24. Gertz M, Tsamandouras N, Sall C, Houston JB, Galetin A. Reduced physiologically-based pharmacokinetic model of repaglinide: Impact of OATP1B1 and CYP2C8 genotype and source of in vitro data on the prediction of drug-drug interaction risk. Pharm Res. 2014;31(9): 2367-82.
25. Neuvonen PJ, Kantola T, Kivisto KT. Simvastatin but not pravastatin is very susceptible to interaction with the CYP3A4 inhibitor itraconazole. Clin Pharmacol Ther. 1998;63(3):332–41.
26. Jacobson TA. Comparative pharmacokinetic interaction profiles of pravastatin, simvastatin, and atorvastatin when coadministered with cytochrome P450 inhibitors. Am J Cardiol. 2004;94(9):1140–6.
27. Son H, Lee D, Lim LA, Jang SB, Roh H, Park K. Development of a pharmacokinetic interaction model for co-administration of simvastatin and amlodipine. Drug Metab Pharmacokinet. 2014;29(2):120–8.
28. Satoh T, Taylor P, Bosron WF, Sanghani SP, Hosokawa M, Du BNL. Current progress on esterases: from molecular structure to function. Drug Metab Dispos. 2002;30(5):488–93.
29. Vree TB, Dammers E, Ulc I, Horkovics-Kovats S, Ryska M, Merkx I. Variable plasma/liver and tissue esterase hydrolysis of simvastatin in healthy volunteers after a single oral dose. Clin Drug Invest. 2001;21(9):643–52.
30. Tubic-Grozdanis M, Hilfinger J, Amidon G, Kim J, Kijek P, Staubach P, et al. Pharmacokinetics of the CYP 3A substrate simvastatin following administration of delayed versus immediate release oral dosage forms. Pharm Res. 2008;25(7):1591–600.
31. Gibiansky L, Gibiansky E, Bauer R. Comparison of Nonmem 7.2 estimation methods and parallel processing efficiency on a target-mediated drug disposition model. J Pharmacokinet Pharmacodyn. 2012;39(1):17–35.
32. Knauer MJ, Urquhart BL, Meyer zu Schwabedissen HE, Schwarz UI, Lemke CJ, Leake BF, et al. Human skeletal muscle drug

transporters determine local exposure and toxicity of statins. Circ Res. 2010;106(2):297–306.
33. Kameyama Y, Yamashita K, Kobayashi K, Hosokawa M, Chiba K. Functional characterization of SLCO1B1 (OATP-c) variants, SLCO1B1*5, SLCO1B1*15 and SLCO1B1*15+C1007G, by using transient expression systems of HeLa and HEK293 cells. Pharmacogenet Genomics. 2005;15(7):513–22.
34. Tomita Y, Maeda K, Sugiyama Y. Ethnic variability in the plasma exposures of OATP1B1 substrates such as HMG-CoA reductase inhibitors: a kinetic consideration of its mechanism. Clin Pharmacol Ther. 2013;94(1):37–51.
35. Lippert J, Brosch M, von Kampen O, Meyer M, Siegmund HU, Schafmayer C, et al. A mechanistic, model-based approach to safety assessment in clinical development. CPT: Pharmacosmet Syst Pharmacol. 2012;1:e13.
36. Rose RH, Neuhoff S, Abduljalil K, Chetty M, Rostami-Hodjegan A, Jamei M. Application of a physiologically based pharmacokinetic model to predict OATP1B1-related variability in pharmacodynamics of rosuvastatin. CPT: Pharmacosmet Syst Pharmacol. 2014;3:e124.
37. Link E, Parish S, Armitage J, Bowman L, Heath S, Matsuda F, et al. SLCO1B1 variants and statin-induced myopathy-a genomewide study. N Engl J Med. 2008;359(8):789–99.
38. Watanabe T, Kusuhara H, Maeda K, Shitara Y, Sugiyama Y. Physiologically based pharmacokinetic modeling to predict transporter-mediated clearance and distribution of pravastatin in humans. J Pharmacol Exp Ther. 2009;328(2):652–62.
39. Chu X, Korzekwa K, Elsby R, Fenner K, Galetin A, Lai Y, et al. Intracellular drug concentrations and transporters: measurement, modeling, and implications for the liver. Clin Pharmacol Ther. 2013;94(1):126–41.
40. Fenneteau F, Poulin P, Nekka F. Physiologically based predictions of the impact of inhibition of intestinal and hepatic metabolism on human pharmacokinetics of CYP3A substrates. J Pharm Sci. 2010;99(1):486–514.
41. Lee AJ, Maddix DS. Rhabdomyolysis secondary to a drug interaction between simvastatin and clarithromycin. Ann Pharmacother. 2001;35(1):26–31.
42. Yeo KR, Yeo WW, Wallis EJ, Ramsay LE. Enhanced cholesterol reduction by simvastatin in diltiazem-treated patients. Br J Clin Pharmacol. 1999;48(4):610–5.
43. Gelman A, Bois F, Jiang J. Physiological pharmacokinetic analysis using population modeling and informative prior distributions. J Am Stat Assoc. 1996;91(436):1400–12.
44. Jonsson F, Jonsson EN, Bois FY, Marshall S. The application of a Bayesian approach to the analysis of a complex, mechanistically based model. J Biopharm Stat. 2007;17(1):65–92.
45. Krauss M, Burghaus R, Lippert J, Niemi M, Neuvonen P, Schuppert A, et al. Using Bayesian-PBPK modeling for assessment of inter-individual variability and subgroup stratification. In Silicon Pharmacol. 2013;1(1):6.
46. Wulkersdorfer B, Wanek T, Bauer M, Zeitlinger M, Muller M, Langer O. Using positron emission tomography to study transporter-mediated drug-drug interactions in tissues. Clin Pharmacol Ther. 2014;96(2):206–13.